IEEE Access
Multidisciplinary | Rapid Review | Open Access Journal

Received April 7, 2020, accepted April 27, 2020, date of publication May 7, 2020, date of current version May 21, 2020.

Digital Object Identifier 10.1109/ACCESS.2020.2993115

A Study of Dynamic Equivalence Using the Similarity Degree of the Equivalent Power Angle in Doubly Fed Induction Generator Wind Farms

LIN ZHU[1], JIAN ZHANG[1], DANTING ZHONG[1], BEI WANG[2], ZHIGANG WU[1], MIN XU[3], AND QING LI[4]

[1]School of Electric Power Engineering, South China University of Technology, Guangzhou 510640, China
[2]State Grid Nantong Electric Power Supply Company, Nantong 226000, China
[3]Electric Power Research Institute of China Southern Power Grid, Guangzhou 510530, China
[4]Maintenance and Test Center, CSG EHV Power Transmission Company, Guangzhou 510530, China

Corresponding author: Lin Zhu (zhul@scut.edu.cn)

This work was supported by the National Natural Science of Foundation of China under Grant U1766213.

ABSTRACT This paper presents a study of dynamic equivalence for doubly fed wind farms (DFWFs) in large power systems. The core idea is to find an attribute representing the critical characteristics of a doubly fed induction generator (DFIG) and use it for clustering in the equivalent modeling process. Using the voltage and flux linkage equations of DFIGs, we derived an electromagnetic power expression. Similar to the power angle concept for synchronous generators, an equivalent power angle (EPA) is proposed and shown to represent the dynamic characteristics of a DFIG in the test system. We introduce the similarity degree of the EPA based on similarity theory and construct a similarity index of the EPA for clustering a DFWF. A practical algorithm was developed for parameter aggregation of the equivalent model. In addition, a simulation of DFWFs in Yunnan, China, was conducted to show the feasibility and high precision of the proposed method.

INDEX TERMS Doubly fed induction generator, equivalent power angle, dynamic equivalent, similarity degree.

I. INTRODUCTION

With the rapid developments in wind power in recent years, the doubly fed induction generator (DFIG) has become a popular type of wind turbine (WT) in most wind farms (WFs) and now plays a prominent role in power systems. WFs usually consist of dozens or even hundreds of WTs, and this leads to tremendous challenges in the dynamic analysis of bulk power systems because detailed models of WFs create an enormous computational burden and are time-consuming. An equivalent model of a doubly fed wind farm (DFWF) substantially reduces the scale while exhibiting similar responses and is powerful enough to fulfil the simulation requirements in the above scenario. Such models have received considerable attention.

Studies have shown some achievements regarding the equivalence of WTs [1]–[10]. Similar to coherency-based dynamic equivalents of synchronous generators, there are two crucial processes in building a reasonable equivalent model of a DFIG: rational clusters and parameter aggregation.

As the most crucial and first step, a rational cluster initiates DFIG WT groups with similar characteristics. The physical properties of wind power are generally chosen as pivotal factors during the clustering process. For example, Ref. [1] and Ref. [2] used wind speeds for coherent identification. Ref. [3] considered the wake effect factor and the action of the blade pitch angle as the classification index for the same WF. However, various operating conditions and the complex properties of wind power, especially wind intermittency and uncertainty, create challenges for these methods.

Considering the composition of DFIGs, researchers have also proposed that converter controllers and crowbar protection should both be used for clustering and aggregation because of the close link with the dynamic characteristics of the DFIG. Based on this idea, [4] developed a refined dynamic equivalent model for a DFWF. However, whether

The associate editor coordinating the review of this manuscript and approving it for publication was Junjian Qi.

this model can meet the simulation requirements for large power grids with a high penetration of wind power, where certain WFs need to be largely reduced, is unclear.

Recently, several artificial algorithms have been applied to clusters of coherent WTs, including the K-means algorithm, the density peak clustering algorithm, and the fuzzy clustering algorithm [5]–[7]. These algorithms provide new insights into the way WTs are processed and clustered. However, the algorithms must be trained with massive datasets, which is time-consuming.

Parameter aggregation is used to identify adequate parameters for an equivalent model and ensure that the accuracy of the dynamic responses is comparable to that of the original system. For instance, the equivalent models of group generators and their optimized parameters can fit aggregated transfer functions within tolerable accuracies, and the dynamics of the active/reactive power and voltage at the point of common coupling (PCC) are consistent with the original system [8]. Ref. [9] proposed an approach in the time domain based on structure preservation, which is more easily implemented than the traditional aggregation method in the frequency domain. Ref. [10] developed a dynamic weighted aggregation equivalent modeling method in which the weighting factors for each generator were calculated according to a Weibull distribution of wind speeds.

Notably, almost all of these studies involved a multi-equivalent model of WTs within the same WF only, ignoring the scenario of equivalent models for various WFs [11]. A multi-equivalent model obtained by the above method can work well for a small-scale power system. In contrast, such a model will not be accepted for the dynamic analysis and security assessment of main power grids in which one must extensively reduce and equalize the generating units, networks, and loads at remote terminals. Considering these circumstances, the aim of this paper is to achieve these goals. A reasonable equivalent method with acceptable accuracies and flexibilities for various WFs is significant and can dramatically reduce the scale and time of the simulations.

To overcome these limitations, this paper proposes a novel method of dynamic equivalence for DFWFs. The core idea of this paper is inspired by the slow coherency and aggregation of synchronous generators that successfully use natural or inherent properties to derive reduced models and obtain the parameters [12]–[15]. The process of coherency and aggregation takes advantage of the power angles of generators after disturbances and identifies groups of coherent generators based on similar swing curves of the generator power angles. Then, models for the equivalent generators and optimized parameters are chosen to fit the aggregated transfer functions within tolerable accuracies. For studies of the dynamic equivalence of DFWFs, the core idea of the aforementioned studies is still attractive, but the following issues must be resolved:

(1) It is critical to find properties that can properly represent the dynamic characteristics of DFWFs.

(2) The proposed method can effectively cluster WFs into various groups with the above properties.

(3) A proper and practical parametrization for the equivalent model must be identified after clustering the WFs.

Using the voltage and flux linkage equations of WFs, we derive the equivalent power angle (EPA) between the equivalent transient internal voltage (ETIV) and the PCC voltage [16]. The EPA represents the dynamic characteristics of a WF, and use of the EPA in the clustering of DFWFs is novel. However, the EPA varies widely with the operational conditions and disturbances and challenges the conventional slow-coherency criterion. This paper introduces the similarity degree of the EPA based on similarity theory and applies the similarity degree to the EPA for clustering. A practical algorithm based on power weights is used to aggregate the parameters of the equivalent model. In addition, time-domain simulations are carried out to validate the proposed method.

II. EQUIVALENT POWER ANGLE AND ITS CHARACTERISTICS

A. DEFINITION OF THE EPA

The dynamic characteristics of a DFIG closely rely on its composition. As shown in Fig. 1, a DFIG mainly consists of an induction generator and two back-to-back converters. Hence, to find a physical quantity that characterizes the operating state of a DFIG, it is necessary to analyze the mathematical model of the induction generator and the back-to-back converter.

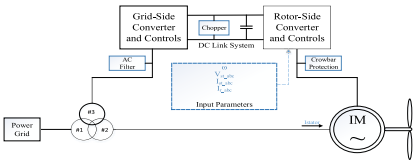

FIGURE 1. Basic structural diagram of a doubly fed wind power generation system.

The voltage equations of the stator and rotor of the DFIG are shown in (1) for the d-q synchronous reference frame:

$$\begin{cases} u_{sd} = R_s i_{sd} + p\psi_{sd} - \psi_{sq} \\ u_{sq} = R_s i_{sd} + p\psi_{sq} + \psi_{sd} \\ u_{rd} = R_r i_{rd} + p\psi_{rd} - s\psi_{rq} \\ u_{rq} = R_r i_{rq} + p\psi_{rq} + s\psi_{rd} \end{cases} \tag{1}$$

where u, i and Ψ represent the voltage, current, and flux linkage of the DFIG, respectively; R is resistance of the DFIG; the subscripts s and r denote the stator and rotor quantities, respectively; p is a differential operator; s is the slip; and the subscripts d and q indicate the direct-axis and the quadrature-axis, respectively.

The flux equations of the stator and rotor are shown in (2):

$$\begin{cases} \psi_{sd} = L_s i_{sd} + L_m i_{rd} \\ \psi_{sq} = L_s i_{sq} + L_m i_{rq} \\ \psi_{rd} = L_m i_{sd} + L_r i_{rd} \\ \psi_{rq} = L_m i_{sq} + L_r i_{rq} \end{cases} \tag{2}$$

where L_m is the mutual inductance.

By combining (1) and (2), the voltage can be written as

$$\begin{cases} u_{sd} = R_s i_{sd} - X_{ss} i_{sq} - \dfrac{L_m}{L_r}\psi_{rq} + p\psi_{sd} \\ u_{sq} = R_s i_{sq} + X_{ss} i_{sd} + \dfrac{L_m}{L_r}\psi_{rd} + p\psi_{sq} \end{cases} \tag{3}$$

where X_{ss} is the equivalent reactance, which is calculated as

$$X_{ss} = L_s - L_m^2 \Big/ L_r \tag{4}$$

The back-to-back converters involve a rotor-side converter (RSC) and a grid-side converter (GSC). Fig. 2 shows the control block diagram of the RSC and GSC.

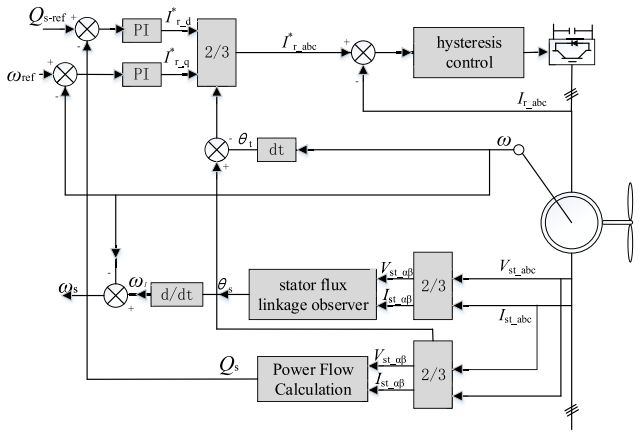

FIGURE 2. The control block diagram of the RSC and GSC.

Using a stator-flux orientation, the RSC provides decoupled control of the active and reactive power, and the GSC is employed to maintain a constant voltage on the DC-link. Fig. 2 shows that the control of the DFIG eventually reflects variables such as the terminal voltage, current, and flux linkage of the DFIG. Thus, we can use these variables to construct E'.

Let

$$\begin{cases} E'_d = -\dfrac{L_m}{L_r}\psi_{rq} + p\psi_{sd} \\ E'_q = \dfrac{L_m}{L_r}\psi_{rd} + p\psi_{sq} \end{cases} \tag{5}$$

where E'represents the voltage under control. Considering $X_{ss} \gg R_s$, the voltage drop on the stator can be ignored, and the ETIV of the DFIG is

$$\boldsymbol{E}' = \boldsymbol{U}_s - \mathrm{j}X_{ss}\boldsymbol{I}_s \tag{6}$$

From (6) we find that the DFIG and synchronous machine have the same form between the transient potential E' and terminal voltage U_s. Similar to the power angle concept from synchronous generators, δ_{dfig} is defined as the EPA, which is the angle between E' and U_s [16], [17]. For the sake of analysis, we let E' be aligned with the q axis to easily obtain the relationships among the power factor angle φ, inner power factor angle θ, and EPA δ_{dfig}, as shown in Fig. 3.

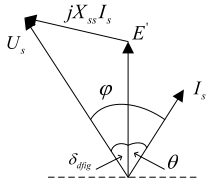

FIGURE 3. Power factor angle and inner power factor angle of the DFIG.

We can derive the output power P_{es} from the stator side of the DFIG:

$$P_{es} = \frac{E'U_s}{X_{ss}} \sin\delta_{dfig} \tag{7}$$

The electromagnetic power P_e can be calculated as

$$P_e = (1-s)\frac{E'U_s}{X_{ss}} \sin\delta_{dfig} \tag{8}$$

In the electromechanical transient process, the DFIG rotor speed changes slowly, and the slip s has little impact on the flux linkage Ψ_t. The rotor flux Ψ_t is decoupled from the mechanical motion of the rotor in the dynamic process. According to (5), the EPA is independent of the physical rotor position but changes in the electromechanical transient process. When a fault occurs, the dynamic characteristics of the DFIG can be triggered, and the EPA may aggravate the consequence caused by the fault [18]. In the next section, we examine an EPA with characteristics that suit the identification of the coherence between DFIGs.

B. CHARACTERISTICS OF THE EPA

In a DFIG, the mechanical part and electrical parts can be decoupled. The WTs, RSC, and GSC mainly affect the output power of the grid-connected bus. There are three types of control modes in the RSC: constant voltage control, reactive power control, and power factor control. We constructed a simple test system to examine the characteristics of the EPA.

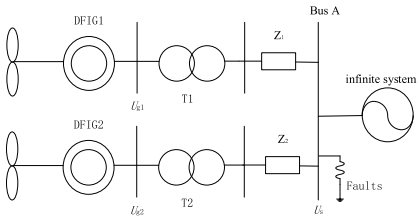

FIGURE 4. Test system.

As shown in Fig. 4, the two DFIGs in the test system can adopt identical or different control strategies. The parameters of T1 and T2 are same. The values of Z_1 and Z_2 are equal. The parameters of the system in Fig. 4 are shown in TABLE 1. The control strategy of DFIG1 is constant voltage control, whereas constant reactive power control is applied in DFIG2. We focus on observing the active power and the

TABLE 1. Parameters of the doubly fed induction generator and controller in the test system.

component	Parameter	Value
DFIG1 DFIG2	nominal power	1.5MW
	nominal voltage	0.69kV
	nominal frequency	50Hz
	stator resistance	0.0054pu
	stator leakage inductance	0.1pu
	rotor resistance	0.00607pu
	rotor leakage inductance	0.11pu
	magnetizing inductance	4.5pu
Z_1 Z_2	line resistance, R_l	0.02 pu
	line reactance, X_l	0.50 pu
T1, T2	transformer reactance	0.14 pu
Crowbar[19-20]	maximum rotor current	2.8pu

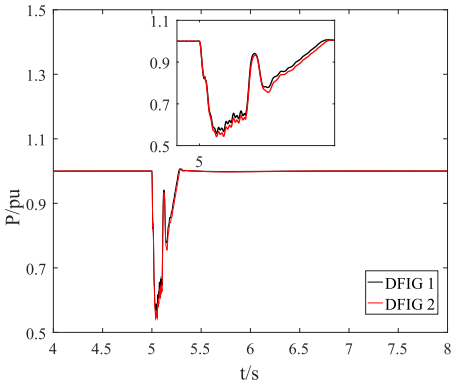

FIGURE 5. Active power of the DFIG with the same control mode.

EPA after a fault occurs. When t=5 s, a single-phase ground fault occurs, which lasts for 0.1 s before removal. Figs. 5-8 present the curves of the active power and EPA in these scenarios.

In Fig. 5 and Fig. 6, under the same control mode, the active powers of the two DFIGs exhibit a similar tendency and amplitude after the faults. This means that two DFIGs should be clustered into a coherent group when the active power and EPA curves of the two DFIGs are consistent. From Fig. 7 and Fig. 8, we can see that the two DFIGs represent different dynamic characteristics under various control modes. However, the EPA shows more apparent and intuitive differences between the two DFIGs. This result reflects the amplification effect of the EPA after the fault. The simulation indicates that taking the EPA as an observable variable for coherent identification is reasonable.

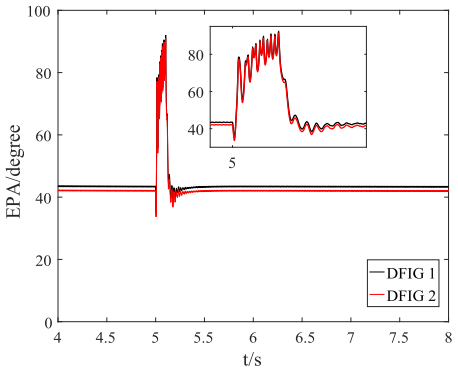

FIGURE 6. Curves of the EPA with the same control mode.

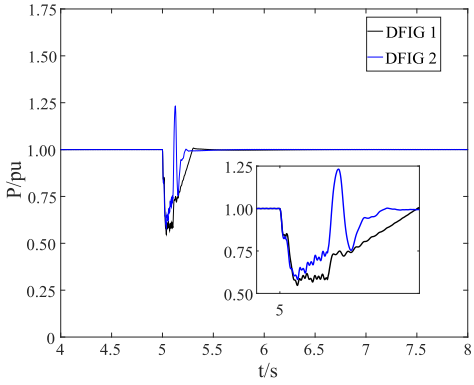

FIGURE 7. Active power of the DFIG with different control modes.

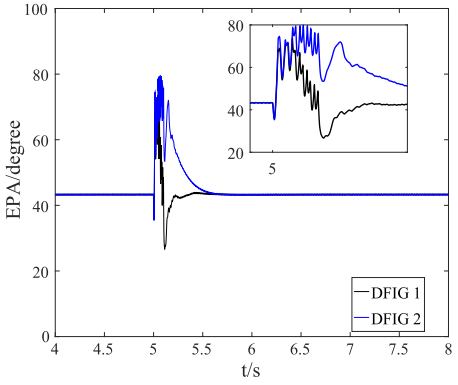

FIGURE 8. Curves of the EPA with different control modes during a fault.

III. AN INDEX OF THE SIMILARITY DEGREE FOR THE EPA

In the previous section, we discussed the derivation and characteristics of the EPA. For a conventional synchronous generator, the swing of the power angles can act as the criterion for coherent identification under different disturbances, as shown in (9).

$$\max_{t\in[0,\tau]} \left|\Delta\delta_i(t) - \Delta\delta_j(t)\right| \leq \varepsilon \tag{9}$$

This conventional criterion cannot apply directly to the EPA because the EPA varies with the operational conditions and disturbances. In this paper, a novel method that fully

utilizes inherent attributes is proposed. Based on similarity theory [21], we employ the Prony algorithm to analyze and extract the properties of the EPA curves, such as the frequency of oscillation and damping ratio, as the Prony algorithm is a commonly used signal processing algorithm [22]. The Prony method uses a linear combination of a set of exponential terms to fit equally spaced sampling data, from which information such as the damping and frequency of the signal can be extracted. We use these properties to construct a similarity index. Finally, we apply the similarity degree to DFIGs and successfully cluster the DFIGs.

A. THE BASIC PRINCIPLE OF SIMILARITY THEORY

Similarity theory can describe the degree of similarity between two objects that are similar in composition or characteristics. Similar elements are units that have common attributes and characteristics between objects with different values. Suppose that object A consists of m elements and that object B has n elements. According to the principle for selection, there are l pairs of similar elements between objects A and B. The degree of similarity between the i^{th} pair of similar elements is $q(ui)$, and the weight of $q(ui)$ is β_{i}. The degree of similarity Q between objects A and B is a function of the above quantities, which can be expressed as:

$$\begin{aligned} Q &= f(m, l, n, q(u_i), \beta_i) \\ i &= 1, 2, \ldots, n \end{aligned} \tag{10}$$

If objects A and B correspond to a curve, the corresponding elements may be the frequency, amplitude, damping, phase, etc., with a total of l. Then, equation (10) can be specified as:

$$Q_{(A,B)} = \sum_{i=1}^{l} \beta_i q(u_i) \tag{11}$$

Artificially setting a threshold ν when $Q_{(A,B)}$ is equal to or greater than ν, A and B can be considered to be similar. Using similarity theory, we can depict the similarity degree of the EPA, which can be used as the coherent clustering criterion for DFIGs.

B. APPLICATION OF SIMILARITY THEORY TO THE EPA

Taking two EPA curves of DFIGs under faults as A and B mentioned above, we use the Prony algorithm to extract the elements of the curves and obtain the elements of the curve in a given order. These elements usually contain many redundant parts with amplitudes close to 0. Therefore, the redundant orders can be eliminated by setting the energy threshold e, which decreases similar elements between the DFIGs. The elimination works as follows: the energies of all elements are ordered from high to low and are summed until the sum is equal to or greater than the product of the total energy $\sum E_{\text{i}}$ and threshold e.

$$\sum_{i=1}^{l} E_i \geq \sum_{i=1}^{n} E_i \times e \tag{12}$$

The contributing orders of the curves for the EPA are confirmed, which are also similar elements between DFIGs A and B. From the simulation in section II, we can conclude that the frequency and damping are the primary factors affecting the tendency of the curves. We think it is more suitable to define the frequency and damping as the frequency of oscillation and the damping ratio, respectively. The damping ratio represents the rate of decay of the amplitude of the EPA curve. Therefore, the i^{th} order similar elements of the frequency and damping between A and B are shown in equations (13) and (14):

$$q(f_i) = 1 - \frac{|f_{Ai} - f_{Bi}|}{f_{Ai}} \tag{13}$$

$$\begin{cases} q(\alpha_i) = 1 - \dfrac{|\alpha_{Ai} - \alpha_{Bi}|}{\alpha_{Ai}}, & \alpha_{Ai} \times \alpha_{Bi} > 0 \\ 0, & \alpha_{Ai} \times \alpha_{Bi} < 0 \end{cases} \tag{14}$$

where f_{i} and α_{i} are the frequency and damping of the i^{th} element of the EPA curves, respectively, and A and B represent the EPA values of DFIGs A and B, respectively.

Considering the similar weight of the frequency and damping, the similarity of the i^{th}similar element is

$$\begin{cases} q(\lambda_i) = \beta_{i1} q(f_i) + \beta_{i2} q(\alpha_i) \\ \beta_{i1} + \beta_{i2} = 1 \end{cases} \tag{15}$$

β_{i1} and β_{i2} are the weights of the frequency and damping, respectively, which can be set according to the actual requirements. Both the damping and frequency represent key characteristics and trends of the EPA curve, so the weights of the two variables are equally important. The parameters can also be determined by trying different values here. According to the practical problem in this paper, the weights of the frequency and damping were set to be equal. Hence, equation (15) can be written as

$$q(\lambda_i) = 0.5 q(f_i) + 0.5 q(\alpha_i) \tag{16}$$

The ratio of the energy of each order to the total energy is defined as follows:

$$\gamma_i = \frac{E_i}{\sum_{i=1}^{l} E_i} \tag{17}$$

Considering the weight, the similarity of all similar elements can be written as

$$Q_f = \sum_{i=1}^{l} (q(\lambda_i) \times \gamma_i) \tag{18}$$

The process of calculating the similarity index under a single fault is given above. Note that the similarity index needs to consider the similarity of the dynamic characteristics of the EPA between the DFIGs under different fault types.

There are k types of faults at the output end of each DFIG. For fault type i, the similarity between the DFIGs can be

calculated as $Q_{f(i)}$, and the similarity index of the coherent identification of different faults is defined as follows:

$$Q_{\mathrm{F}} = \frac{1}{k}\sum_{i=1}^{k} Q_{f(\mathrm{i})} \tag{19}$$

Through calculation of the similarity index between the DFIGs, the coherent DFIGs in the WF are determined.

IV. AGGREGATION OF THE COHERENT DFIGS

After clustering the WFs, we introduce a practical algorithm based on the weighting factors of the DFIG active powers. Considering that WFs in the same cluster are parallel to each other at the aggregated bus, parameters of the equivalent WT are easily obtained from this topology.

A. AGGREGATION OF THE COHERENT BUS

There are N DFIGs in the coherent group, and the ETIV is

$$\boldsymbol{E}'_{\mathrm{equ}} = \frac{\sum_{l=1}^{N} p_l \boldsymbol{E}'_l}{\sum_{l=1}^{N} p_l} \tag{20}$$

where E'_{equ} is the ETIV of the equivalent WT; P_{l} is the active power of the i^{th} DFIG; and E'_{l} is the ETIV of the l^{th} DFIG.

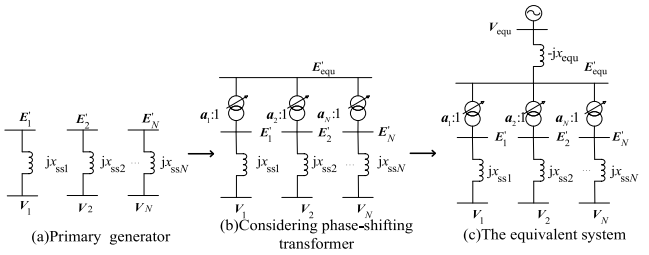

FIGURE 9. The procedure of creating an equivalent generator.

E'_{l} is connected to E'_{equ} through a complex variable ratio phase-shifting transformer (shown in Fig. 9 (b)) with a ratio of

$$\boldsymbol{a}_l = \frac{\boldsymbol{E}'_{\mathrm{equ}}}{\boldsymbol{E}'_l} \tag{21}$$

According to equation (22), the equivalent bus of the DFIG can be determined by the ETIV and the equivalent reactance (shown in Fig. 9 (c)). The equivalent reactance is

$$X_{\mathrm{equ}} = X_{\mathrm{ss1}} // X_{\mathrm{ss2}} // \cdots // X_{\mathrm{ssN}} \tag{22}$$

where X_{ssN} is the equivalent reactance of the N^{th} DFIG.

Because large-capacity WTs in WFs have a greater influence on the dynamic characteristics of the system than other WTs, the dynamic characteristics of WFs can be better maintained if the aggregation takes the active power output of the WT as the weight rather than using the mean value method.

B. PARAMETER AGGREGATION OF AN EQUIVALENT WIND TURBINE

The rated capacity and output characteristics of the coherent groups should remain consistent with those of the original system. Therefore, the parameters of the equivalent WT are

$$\begin{cases} P_{\mathrm{eq}} = \sum_{i=1}^{N} P_i \\ Q_{\mathrm{eq}} = \sum_{i=1}^{N} Q_i \\ X_{\mathrm{seq}} = X_{\mathrm{s1}} // X_{\mathrm{s2}} // \cdots // X_{\mathrm{sN}} \\ X_{\mathrm{req}} = X_{\mathrm{r1}} // X_{\mathrm{r2}} // \cdots // X_{\mathrm{rN}} \\ R_{\mathrm{req}} = R_{\mathrm{r1}} // R_{\mathrm{r2}} // \cdots // R_{\mathrm{rN}} \\ R_{\mathrm{seq}} = R_{\mathrm{s1}} // R_{\mathrm{s2}} // \cdots // R_{\mathrm{sN}} \end{cases} \tag{23}$$

where P is the active power, and Q is the reactive power. The subscripts eq represent the parameters of the equivalent WT.

For calculation of the shafting parameters of the equivalent WT, a method similar to that for solving the ETIV is adopted. Therefore, the shafting parameters of the equivalent WT are

$$\begin{cases} H_{\mathrm{geq}} = \dfrac{\sum_{i=1}^{N} p_i H_{\mathrm{g}i}}{\sum_{i=1}^{N} p_i} \\ H_{\mathrm{teq}} = \dfrac{\sum_{i=1}^{N} p_i H_{\mathrm{t}i}}{\sum_{i=1}^{N} p_i} \\ K_{\mathrm{seq}} = \dfrac{\sum_{i=1}^{N} p_i K_{\mathrm{s}i}}{\sum_{i=1}^{N} p_i} \end{cases} \tag{24}$$

where H_{gi}, H_{ti}, and H_{si} represent the inertia time constant, the inertia time constant of the rotor of the WT, and the stiffness coefficient of the shafting of the i^{th} generator, respectively.

V. CASE STUDY

We take a grid integrated with WFs in Yunnan province, China, as a case study. This small part of the Yunnan power grid with concentrated wind power is selected to verify the equivalent effect in DFWFs. There are 17 DFWFs in this system, as shown in Fig. 10. To avoid excessive equivalent lines, preliminary groups are necessary. These clustering groups usually depend on the connected buses and electrical distance. Thus, the preliminary results of clustering for these WFs can be obtained as WF1 = [YISG1, YISG2, FETUG1,

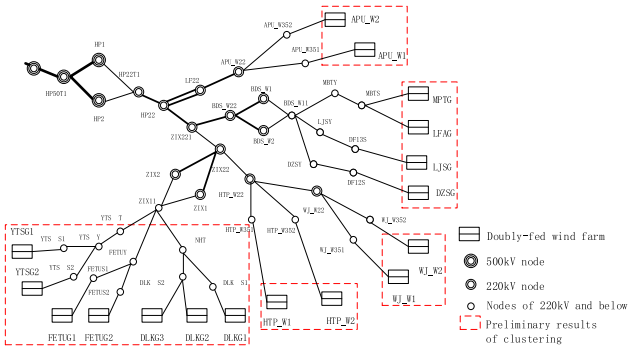

FIGURE 10. Geographical wiring diagram of WFs in the Yunnan power grid.

FETUG2, DLKG3, DLKG2, DLKG1]; WF2 = [HTP_W1, HTP_W2]; WF3 = [WJ_W1, WJ_W2]; WF4 = [MPTG, LFAG, LJSG, DZSG]; and WF5 = [APU_W1,APU_W2]. Based on the EPA and the proposed similarity degree, a more accurate coherency identification is achieved in the following section.

A. MEASUREMENT OF THE EPA

Two types of faults (a three-phase fault and a single-phase ground fault) are set on the PCC of the WFs. We show the results for the case when a three-phase fault occurs in line HP22-HP22T1 at 5 s and disappears at 5.1 s. The curves of the EPA for the DFWFs are shown in Figs. 11-15.

From the simulations of the two types of faults and Figs. 11-15, we find that the DFIGs in WF2, WF3, and WF5 are coherent due to their identical dynamics. However, modifications should be made to WF1 and WF4. In WF1,

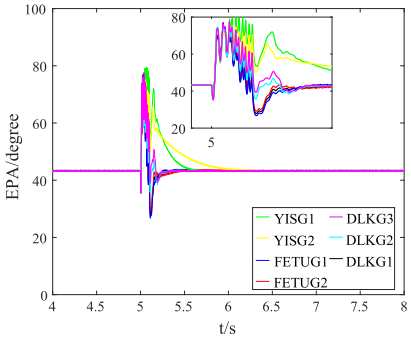

FIGURE 11. The EPA of the DFIGs in WF1.

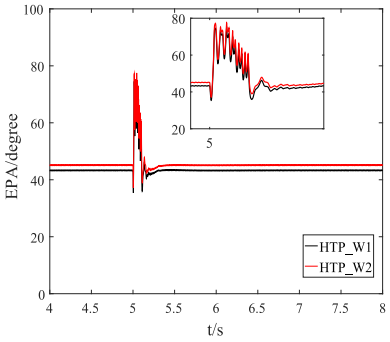

FIGURE 12. The EPA of the DFIGs in WF2.

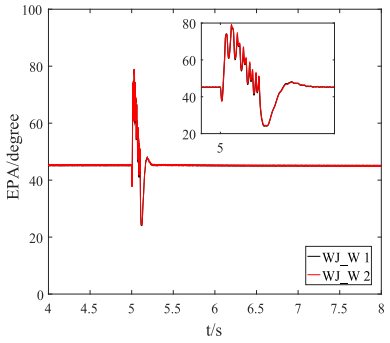

FIGURE 13. The EPA of the DFIGs in WF3.

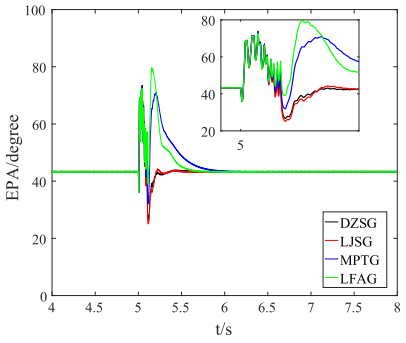

FIGURE 14. The EPA of the DFIGs in WF4.

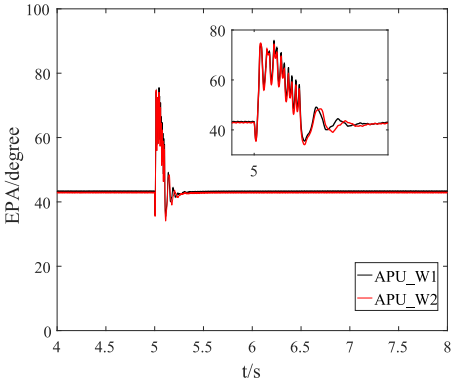

FIGURE 15. The EPA of the DFIGs in WF5.

FETUG1, FETUG2, and DLKG1 are similar and should be coherent in one group, whereas YISG1 and YISG2 and DLKG2 and DLKG3 consist of the second and third groups, respectively. Similar modifications should be made for WF4; MPTG and LFAG should be grouped, and LJSG and DZSG are coherent. The final clustering can be confirmed by the similarity degree.

B. COHERENCY IDENTIFICATION BASED ON THE SIMILARITY INDEX

Through observation of the EPA results, some curves do not quantitatively identify the coherency. Thus, the EPA curve under contingencies is used to extract a series of data. The data are used to calculate the similarity index between the DFIGs. If the similarity index of the EPA Q_{EPA} is 0.85 or greater, the two DFIGs are coherent. The results of the calculation are shown in Tables 2 - 4.

From the results of Tables 2 - 4, we can obtain the final clustering with the similarity index. The pro-fault power curves are shown to verify the validity of the clustering results. Figs. 16-19 show the active power output of the WT under contingencies. Fig. 16 shows that the coherence between FETUG1 and FETUG2 is better than that of the FETUG1 and DLKG1 group, which is in accordance with the results in Table 2. These WFs were divided into 8 coherent groups, meaning that the number of WFs decreased by 53% in this case. Applying this method for the entire power grid in Yunnan province, we would obtain similar reduction effects.

TABLE 2. Results of the coherency identification in WF1 based on the data analysis method.

DFIG	Q_{EPA}	Coherency identification
(FETUG1, FETUG2)	0.927	yes
(FETUG1, DLKG1)	0.903	yes
(DLKG1, DLKG2)	0.365	no
(DLKG1, YISG1)	0.216	no
(YISG1, YISG2)	0.901	yes
(DLKG2, DLKG3)	0.947	yes

TABLE 3. Results of the coherency identification in WF4 based on the data analysis method.

DFIG	Q_{EPA}	Coherency identification
(LJSG, DZSG)	0.954	yes
(LJSG, MPTG)	0.258	no
(MPTG, LFAG)	0.881	yes

TABLE 4. Results of the coherency identification in WF2, WF3 and WF5 based on the data analysis method.

DFIG	Q_{EPA}	Coherency identification
(HTP_W1,HTP_W2)	0.935	yes
(WJ_W1,WJ_W2)	0.980	yes
(APU_W1,APU_W2)	0.953	yes

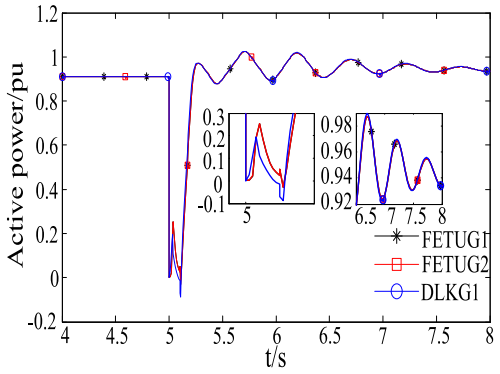

FIGURE 16. Disturbed trajectories of the active power of FETUG1, FETUG2, and DLKG1.

The simulation further illustrates that methods based on the similarity degree of the EPA are feasible and very precise.

C. PARAMETER AGGREGATIONS OF THE COHERENT GROUP

After coherent identifications, we carried out the following parameter aggregations. We compared the proposed algorithm

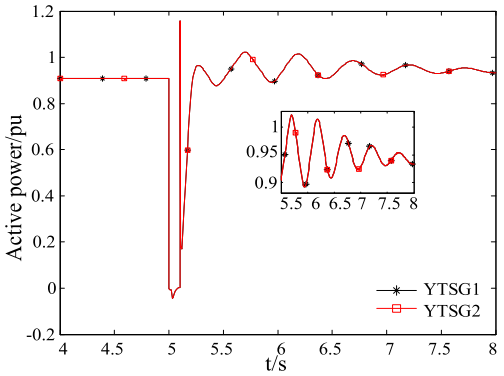

FIGURE 17. Disturbed trajectories of the active power of YTSG1 and YTSG2.

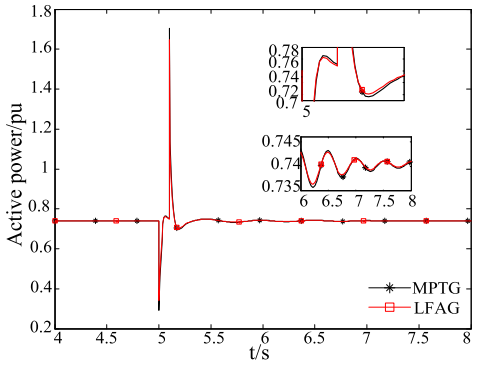

FIGURE 18. Disturbed trajectories of the active power of MPTG and LFAG.

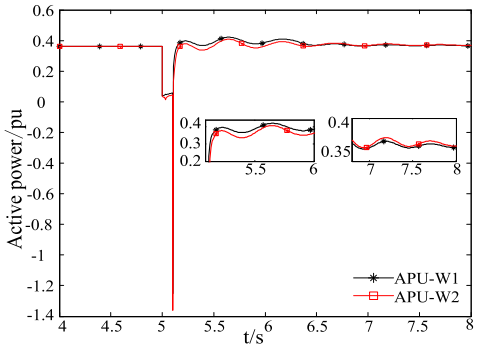

FIGURE 19. Disturbed trajectories of the active power of APU_W1 and APU_W2.

in this paper with a traditional algorithm, the average algorithm, as shown in Fig. 20. We aggregated two DFIGs in WF2 with different capacities. The main parameters of the DFIGs in the test system are shown in Table 5.

Fig. 20 compares the proposed algorithm with the average algorithm through the active power of line APU_W22-LF22. The curve of the power aggregation algorithm is closer to that of the original system, which indicates the superiority of our algorithm.

D. EQUIVALENT EFFECT VERIFICATION

After equivalences, the number of WFs decreased by 53% in the equivalent system compared with the original. Figs. 21-23 show the results of the clustering and aggregation algorithm

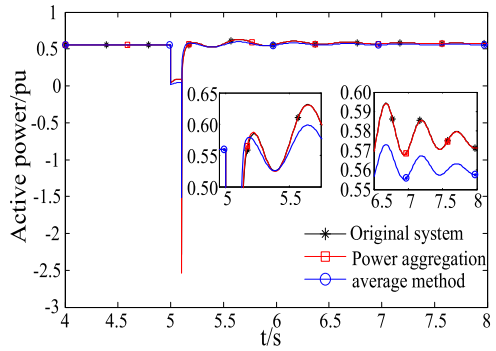

FIGURE 20. Active power of APU_W22-LF22 in the test system.

TABLE 5. The main parameters of the DFIGS in WF5 using power aggregation.

Parameters	APU_W1	APU_W2	Power aggregation
Rated Power	1.5MW	1.0MW	2.5MW
R_s	0.023p.u.	0.01p.u.	0.0069p.u.
R_r	0.016p.u.	0.009p.u.	0.0057p.u.
L_m	2.9p.u.	4.15p.u.	1.7065p.u.
L_s	0.18p.u.	0.06p.u.	0.045p.u.
L_r	0.16p.u.	0.16p.u.	0.16 p.u.
H_t	4.32s	3.86s	4.136s
H_g	0.685s	0.543s	0.6282s
K_s	1.11pu/rad	1.06pu/rad	1.19pu/rad

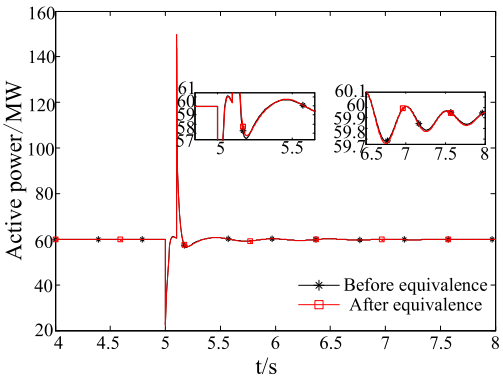

FIGURE 21. Active power of line WJ_W22-HTP_W22.

proposed in this paper. Comparisons of the active power, reactive power, and voltage between the original system and the equivalent system demonstrate that the systems are almost identical. This result also indicates that the proposed method can maintain the dynamic characteristics of the original system. Therefore, the clustering and aggregation method proposed in this paper is reasonable and has a high precision. There are approximately 132 WFs in the Yunnan power grid. Using the proposed method, the scale of the power grid can be reduced while retaining high fidelity. The equivalent system

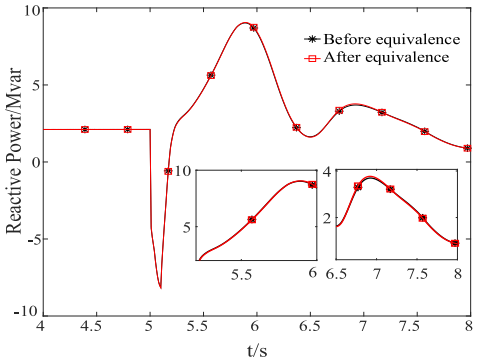

FIGURE 22. Reactive power of line HTP_W22-ZIX22.

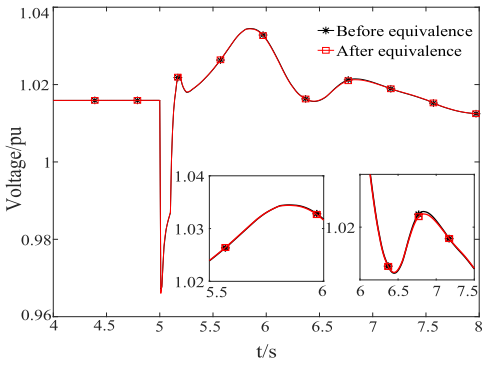

FIGURE 23. Voltage of bus ZIX22.

will save time in the modeling and simulation of dynamic analysis.

VI. CONCLUSION

To reduce the main power grid for dynamic analysis and security assessments, this paper presents a study of the dynamic equivalence for DFWFs. The EPA, the angle between the equivalent transient internal voltage (ETIV) and the PCC voltage, can represent the critical characteristics of a DFIG. Thus, we can introduce the similarity degree of the EPA based on similarity theory to cluster DFWFs. A similarity index of the EPA is used as the criterion for coherent identification. The power weight algorithm can be used to obtain aggregate parameters for the equivalent model. The case study verifies the reduction effect and precision of the method compared with the original system. The simulation results for DFWFs in Yunnan province, China, show the feasibility and high precision of the proposed method.

REFERENCES

[1] Z. Meng, F. Xue, and X. Li, "Wind speed equalization-based incoming wind classification by aggregating DFIGs," *J. Mod. Power Syst. Clean Energy*, vol. 1, no. 1, pp. 42–48, Jun. 2013.
[2] K. Rudion, "Aggregated modelling of wind farms," Ph.D. dissertation, Dept. Elect. Eng., Otto von Guericke Univ. Magdeburg, Magdeburg, Germany, 2008.
[3] J. Tian, D. Zhou, C. Su, Z. Chen, and F. Blaabjerg, "Reactive power dispatch method in wind farms to improve the lifetime of power converter considering wake effect," *IEEE Trans. Sustain. Energy*, vol. 8, no. 2, pp. 477–487, Apr. 2017.
[4] O. Jinxin, D. Yanbo, Z. Di, Y. Rui, Z. Xi, and X. Xiaofu, "Dynamic equivalent model of doubly fed wind farm during electromagnetic transient process," *IET Renew. Power Gener.*, vol. 11, no. 1, pp. 100–106, Jan. 2017.

[5] J. Zou, C. Peng, H. Xu, and Y. Yan, "A fuzzy clustering algorithm-based dynamic equivalent modeling method for wind farm with DFIG," *IEEE Trans. Energy Convers.*, vol. 30, no. 4, pp. 1329–1337, Dec. 2015.

[6] M. Liu, W. Pan, Y. Zhang, K. Zhao, S. Zhang, and T. Liu, "A dynamic equivalent model for DFIG-based wind farms," *IEEE Access*, vol. 7, pp. 74931–74940, 2019.

[7] C. Shuyong, W. Cong, and S. Hong, "Dynamic equivalence for wind farms based on clustering algorithm," (in Chinese), *Proc. CSEE*, vol. 32, no. 4, pp. 11–18, 2012,

[8] H. Zhou, P. Ju, Y. Xue, and J. Zhu, "Probabilistic equivalent model of DFIG-based wind farms and its application in stability analysis," *J. Mod. Power Syst. Clean Energy*, vol. 4, no. 2, pp. 248–255, Apr. 2016.

[9] A. A. M. Zin, B. C. Kok, M. W. Mustafa, K. L. Lo, and A. E. Ariffin, "Time domain dynamic aggregation of generating unit based on structure preserving approach," in *Proc. Nat. Power Eng. Conf. (PECon)*, Bangi, Malaysia, Dec. 2003, pp. 154–160.

[10] Y. Zhou, L. Zhao, I. B. M. Matsuo, and W.-J. Lee, "A dynamic weighted aggregation equivalent modeling approach for the DFIG wind farm considering the weibull distribution," in *Proc. IEEE/IAS 55th Ind. Commercial Power Syst. Tech. Conf. (I&CPS)*, Calgary, AB, Canada, May 2019, pp. 1–7.

[11] J. Brochu, C. Larose, and R. Gagnon, "Validation of single- and multiple-machine equivalents for modeling wind power plants," in *Proc. IEEE Power Energy Soc. Gen. Meeting*, Detroit, MI, USA, Jul. 2011, p. 1.

[12] Y. Jin, D. Wu, P. Ju, C. Rehtanz, F. Wu, and X. Pan, "Modeling of wind speeds inside a wind farm with application to wind farm aggregate modeling considering LVRT characteristic," *IEEE Trans. Energy Convers.*, vol. 35, no. 1, pp. 508–519, Mar. 2020.

[13] J. H. Chow, R. Galarza, P. Accari, and W. W. Price, "Inertial and slow coherency aggregation algorithms for power system dynamic model reduction," *IEEE Trans. Power Syst.*, vol. 10, no. 2, pp. 680–685, May 1995.

[14] H. J. Chow and J. J. Sanchez-Gasca, "Power system coherency and model reduction," in *Proc. Power Syst. Modeling, Comput., Control*, 2020, pp. 531–562.

[15] D. Romeres, F. Dorfler, and F. Bullo, "Novel results on slow coherency in consensus and power networks," in *Proc. Eur. Control Conf. (ECC)*, Zurich, Switzerland, Jul. 2013, pp. 742–747.

[16] M. Zhao, X. Yuan, and J. Hu, "Modeling of DFIG wind turbine based on internal voltage motion equation in power systems phase-amplitude dynamics analysis," *IEEE Trans. Power Syst.*, vol. 33, no. 2, pp. 1484–1495, Mar. 2018.

[17] Z. Cui, X. Yuan, and M. Zhang, "Wind farm aggregation method based on motion equation concept: A case study," *J. Eng.*, vol. 2017, no. 13, pp. 708–713, Jan. 2017.

[18] Z. Ye, Z. Zaiwei, Z. Ling, S. Xiaofang, and X. Feng, "Transient power angle stability analysis of emergency wind turbine tripping," in *Proc. Int. Conf. Renew. Power Gener. (RPG)*, Beijing, China, 2015, pp. 1–6.

[19] Z. Din, J. Zhang, Y. Zhu, Z. Xu, and A. El-Naggar, "Impact of grid impedance on LVRT performance of DFIG system with rotor crowbar technology," *IEEE Access*, vol. 7, pp. 127999–128008, 2019.

[20] H. Xu, J. Hu, and Y. He, "Integrated modeling and enhanced control of DFIG under unbalanced and distorted grid voltage conditions," *IEEE Trans. Energy Convers.*, vol. 27, no. 3, pp. 725–736, Sep. 2012.

[21] Z. Wang, J. Li, K. Fan, W. Ma, and H. Lei, "Prediction method for low speed characteristics of compressor based on modified similarity theory with genetic algorithm," *IEEE Access*, vol. 6, pp. 36834–36839, 2018.

[22] J. F. Hauer, "Application of prony analysis to the determination of modal content and equivalent models for measured power system response," *IEEE Trans. Power Syst.*, vol. 6, no. 3, pp. 1062–1068, Aug. 1991.

LIN ZHU received the Ph.D. degree from the South China University of Technology (SCUT), Guangzhou, China, in 2007. Since 2007, he has been an Associate Professor with the School of Electrical Power Engineering, SCUT. His research interests are in HVDC, power systems, and power system modeling, stability and control.

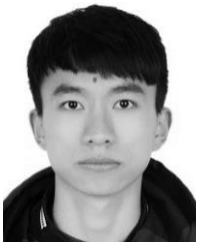

JIAN ZHANG received the B.S. degree from Central South University (CSU), Changsha, China, in 2018. He is currently pursuing the M.S. degree with the School of Electrical Power Engineering, South China University of Technology (SCUT). His research interests are in power system stability and artificial intelligence.

DANTING ZHONG received the B.S. degree in electrical engineering from the South China University of Technology (SCUT), Guangzhou, China, in 2018, where she is currently pursuing the M.S. degree in power system and its automation. Her research interests are in HVDC, wind farm, and power system stability and control.

BEI WANG received the M.S. degree from the South China University of Technology (SCUT), Guangzhou, China, in 2019. His research interests are in HVDC, power system stability and control, and wind power.

ZHIGANG WU was born in Jilin, China, in 1975. He received the bachelor's, master's, and Ph.D. degrees in electrical engineering from Tianjin University, Tianjin, China, in 1996, 1998, and 2002, respectively. He is currently an Associate Professor with the School of Electric Power Engineering, South China University of Technology, Guangzhou, China. His current research interests include power system numerical simulation technology and application of complex network theory in power systems.

MIN XU received the Ph.D. degree from the South China University of Technology (SCUT), Guangzhou, China, in 2014. He is currently a Senior Engineer with the Electric Power Research Institute of China Southern Power Grid. His research interests are in power system stability and control, HVDC, and distribution networks.

QING LI received the Ph.D. degree from the South China University of Technology (SCUT), Guangzhou, China, in 2015. He is currently a Senior Engineer with the Maintenance and Test Center, CSG EHV Power Transmission Company. His research interests are mainly in HVDC control and protection system optimization and ac/dc system interactions analysis.